Two-year longitudinal monitoring of amnestic mild cognitive impairment patients with prodromal Alzheimer's disease using topographical biomarkers derived from functional magnetic resonance imaging and electroencephalographic activity

Jorge Jovicich, Claudio Babiloni, Clarissa Ferrari, Moira Marizzoni, Davide Moretti, Claudio del Percio, Roberta Lizio, Susanna Lopez, Samantha Galluzzi, Diego Albani, et al.

Submitted to Journal of Alzheimer's disease on 13rd of February 2018

Two-year longitudinal monitoring of amnestic mild cognitive impairment patients with prodromal Alzheimer's disease using topographical biomarkers derived from functional magnetic resonance imaging and electroencephalographic activity

Jorge Jovicich[1*], Claudio Babiloni[2,3*], Clarissa Ferrari[4], Moira Marizzoni[5], Davide V. Moretti[6], Claudio Del Percio[7], Roberta Lizio[2], Susanna Lopez[2], Samantha Galluzzi[5], Diego Albani[8], Libera Cavaliere[5], Ludovico Minati[1], Mira Didic[9,10], Ute Fiedler[11], Gianluigi Forloni[8], Tilman Hensch[11], José Luis Molinuevo[12], Flavio Nobili[13], Daniele Orlandi[5], Lucilla Parnetti[14], Lucia Farotti[14], Lucia Costa[14], Pierre Payoux[15], Paolo Maria Rossini[16], Camillo Marra[16], Peter Schönknecht[11], Andrea Soricelli[7], Giuseppe Noce[7], Magda Tsolaki[17], Pieter Jelle Visser[18], Jill C Richardson[19], Jens Wiltfang[20,21,22], Régis Bordet[23], Olivier Blin[24], Giovanni B. Frisoni[5,25] and the PharmaCog Consortium.

[*] Equally contributing Authors

[1] Center for Mind/Brain Sciences, University of Trento, Italy;

[2] Department of Physiology and Pharmacology "V. Erspamer", Sapienza University of Rome, Rome, Italy;

[3] Department of Neuroscence, IRCCS-Hospital San Raffaele Pisana of Rome and Cassino, Rome and Cassino, Italy;

[4] Unit of Statistics, IRCCS Istituto Centro San Giovanni di Dio Fatebenefratelli, Brescia, Italy;

[5] Laboratory of Neuroimaging and Alzheimer's Epidemiology, IRCCS Istituto Centro San Giovanni di Dio Fatebenefratelli, Brescia, Italy;

[6] Alzheimer's Epidemiology and Rehabilitation in Alzheimer's disease Operative Unit, IRCCS Istituto Centro San Giovanni di Dio Fatebenefratelli, Brescia, Italy;

[7] IRCCS SDN Istituto di Ricerca Diagnostica e Nucleare, Napoli, Italy;

[8] Department of Neuroscience, IRCCS - Istituto di Ricerche Farmacologiche Mario Negri, Milano, Italy;

[9] Aix-Marseille Université, INSERM, INS UMR_S 1106, 13005, Marseille, France; Service de Neurologie et Neuropsychologie, APHM Hôpital Timone Adultes, Marseille, France;

[10] APHM, Timone, Service de Neurologie et Neuropsychologie, APHM Hôpital Timone Adultes, Marseille, France;

[11] Department of Psychiatry and Psychotherapy, University of Leipzig, Leipzig, Germany, Germany;

[12] Alzheimer's Disease Unit and Other Cognitive Disorders Unit, Hospital Clínic de Barcelona, and Institut d'Investigacions Biomèdiques August Pi i Sunyer (IDIBAPS), Barcelona, Catalunya, Spain;

[13] Clinical Neurology, Dept. of Neuroscience (DINOGMI), University of Genoa and IRCCS AOU San Martino-IST, Genoa, Italy;

[14] Clinica Neurologica, Università di Perugia, Ospedale Santa Maria della Misericordia, Perugia, Italy;

[15] INSERM; Imagerie cérébrale et handicaps neurologiques UMR 825; F-31059 Toulouse, France;

[16] Department of Gerontology, Neurosciences & Orthopedics, Catholic University, Policlinic A. Gemelli Foundation, Rome, Italy;

[17] 1st University Department of Neurology, Neurologic Clinic, Medical School, G. Papanikolaou Hospital, Aristotle University of Thessaloniki, Thessaloniki, Greece;

[18] Department of Neurology, Alzheimer Centre, VU Medical Centre, Amsterdam, The Netherlands;

[19] Neurosciences Therapeutic Area, GlaxoSmithKline R&D, Gunnels Wood Road, Stevenage, United Kingdom;

[20] LVR-Hospital Essen, Department of Psychiatry and Psychotherapy, Faculty of Medicine, University of Duisburg-Essen, Essen, Germany;

[21] Department of Psychiatry and Psychotherapy, University Medical Center (UMG), Georg-August-University, Goettingen, Germany;

[22] iBiMED, Medical Sciences Department, University of Aveiro, Aveiro, Portugal;

[23] University of Lille, Inserm, CHU Lille, U1171 - Degenerative and vascular cognitive disorders, F-59000 Lille, France;

[24] Aix Marseille University, UMR-CNRS 7289, Service de Pharmacologie Clinique, AP-HM, Marseille, France;

[25] Memory Clinic and LANVIE - Laboratory of Neuroimaging of Aging, University Hospitals and University of Geneva, Geneva, Switzerland.

Keywords: Prodromal Alzheimer’s Disease; Amnesic Mild Cognitive Impairment (aMCI); Functional Magnetic Resonance Imaging (fMRI); Electroencephalography (EEG); Resting State, Alpha rhythms; Oddball Event-Related Potentials (ERPs); Clinical Trial; Biomarkers; PharmaCog project.

Corresponding Authors:

Dr. Jorge Jovicich (section of resting state functional magnetic resonance imaging biomarkers)

Center for Mind/Brain Sciences, University of Trento, Trento, Italy

Phone: +39-0461-28 3064

Fax: +39-0461-28-3066

Email: jorge.jovicich@unitn.it

and

Dr. Claudio Babiloni (section of electroencephalographic biomarkers)

Department of Physiology and Pharmacology "Erspamer", University of Rome "La Sapienza", Rome, Italy

Phone: +39-0649910989

Fax: +39-0649910917

Email: claudio.babiloni@uniroma1.it

Abstract

Auditory "oddball" event-related potentials (aoERPs), resting state functional magnetic resonance imaging (rsfMRI) connectivity and electroencephalographic (rsEEG) rhythms were tested as longitudinal functional biomarkers of prodromal Alzheimer's disease (AD). Data were collected at baseline and four follow-ups at 6, 12, 18, and 24 months in amnesic mild cognitive impairment (aMCI) patients classified in two groups: "positive" (i.e., "prodromal AD"; N=81) or "negative" (N=63) based on a diagnostic marker of AD derived from cerebrospinal samples (Aβ42/P-tau ratio). A linear mixed model design was used to test functional biomarkers for Group, Time, and Group x Time effects adjusted by nuisance covariates (only data until conversion to dementia was used). Functional biomarkers that showed significant Group effects ("positive" vs. "negative", $p<0.05$) regardless of Time were (1) reduced rsfMRI connectivity in both the default mode network (DMN) and the posterior cingulate cortex (PCC), both also giving significant Time effects (connectivity decay regardless of Group); (2) increased rsEEG source activity at delta (< 4 Hz) and theta (4-8 Hz) rhythms and decreased source activity at low-frequency alpha (8-10.5 Hz) rhythms; and (3) reduced parietal and posterior cingulate source activities of aoERPs. Time x Group effects showed differential functional biomarker progression between groups: (1) increased rsfMRI connectivity in the left parietal cortex of the DMN nodes, consistent with compensatory effects, and (2) increased limbic source activity at theta rhythms. These findings represent the first longitudinal characterization of functional biomarkers of prodromal AD relative to "negative" aMCI patients based on 5 serial recording sessions over 2 years.

1. Introduction

The International Working Group has recently made a useful distinction between diagnostic and topographical biomarkers of Alzheimer's disease (AD) for research applications in patients with amnesic mild cognitive impairment (aMCI) due to the prodromal manifestation of the pathology [1]. Diagnostic biomarkers were defined as those measuring *in-vivo* intrinsic pathophysiological variables characterizing neurobiologically AD, namely amyloid deposition and neurofibrillary tangles in the brain. They are expected to be present at all stages of the disease, are observable even in the preclinical asymptomatic state, are not necessarily correlated with disease severity, and are indicated for inclusion of AD patients in clinical trial protocols. Diagnostic biomarkers include low doses of Aβ1–42 and high doses of total tau (T-tau) or phospho tau (P-tau) in cerebrospinal fluid (CSF) or evidence of significant amyloid deposition and tau aggregation in the brain in maps of positron emission tomography (PET) [2].

In contrast, topographic or progression biomarkers may not be specific of AD neuropathology or absent in early disease stages, but they can be very useful to monitor the progression of the disease in the brain and may be related to the kind and severity of cognitive deficits [1]. Progression markers include hippocampal atrophy or cortical thickness, assessed by structural MRI, and cortical hypometabolism in posterior cingulate, parietal, temporal, and hippocampal regions, measured by FDG-PET [1]. Of note, these topographic biomarkers are limited in the sense that they do not directly measure brain amyloid deposition and neurofibrillary tangles in AD patients, so they cannot be used as primary neuropathological endpoints in the evaluation of AD-modifying agents.

Promising candidates as topographic markers of AD are those reflecting functional aspects of brain neurotransmission and connectivity, as human cognition is the result of collective and coordinated behavior of brain networks. In this line, functional MRI accompanying resting state condition (rsfMRI) allows the computation of intrinsic hemodynamic low-frequency (< 1 Hz) statistical correlations of blood oxygenation level dependent (BOLD) signals between brain regions as a marker of brain functional connectivity [3,4]. The default mode network (DMN), which includes posterior and anterior cingulate areas, angular gyri, occipital, and parietotemporal regions, is a particularly relevant network to actively maintain resting state condition in low vigilance and self-awareness [5]. Several studies have shown a significant reduction of DMN brain connectivity in groups of patients with aMCI and AD dementia compared with control seniors with intact cognition [6–11]. As

topographic biomarker of progression, these fMRI biomarkers pointed to a reduction of brain functional connectivity in DMN in aMCI and AD patients with dementia at about 1-year follow up [7,8,12,13].

Other candidate topographic biomarkers of AD derive from electroencephalographic (EEG) techniques, which are noninvasive, cost-effective, and can be repeated several times along disease progression without learning effects affecting paradigms using tasks. When compared to fMRI and FDG-PET, EEG techniques have a modest spatial resolution of some centimeters but a very high temporal resolution (milliseconds); that temporal resolution is ideal to investigate brain rhythms during resting state condition (i.e. resting state EEG, rsEEG) and quick brain dynamics in response to cognitive-motor events challenging attention and short episodic memory (i.e., event-related potentials, ERPs). Derived rsEEG/ERP biomarkers may reflect synchronization and connectivity between large populations of cortical pyramidal neurons in resting state conditions or during cognitive tasks [14]. Previous studies have shown that compared to control seniors, patients with aMCI and dementia due to AD were characterized by increased rsEEG power density at delta (< 4 Hz) and theta (4-7 Hz) frequency bands in widespread cortical regions as well as decreased rsEEG power density at alpha (8-13 Hz) and beta (14-30 Hz) frequency bands in central and posterior cortical regions [6,14–23]. Furthermore, these patients were also characterized by latency increase and amplitude decrease in late positive parietal ERPs (i.e., P3b) peaking at about 300-400 ms from the onset of a rare (20-30% of probability to occur in a sequence with frequent auditory stimuli to be ignored) auditory or visual stimulus triggering hand motor responses or mental stimulus counting [24–29]. As topographic biomarkers of progression, these EEG/ERP readouts pointed to increased abnormalities in delta/alpha rhythms and P3b peak in aMCI and AD patients with dementia at about 1-year follow up [17,18,25,27]. These effects were typically discussed in relationship to death of cortical neurons, axonal pathology, and cholinergic neurotransmission deficits [19,30–36].

The mentioned findings motivate the evaluation of rsfMRI and rsEEG/P3b as topographic biomarkers sensitive to prodromal (MCI) and dementia stages of AD. This process needs to overcome the following methodological limitations of typical multi-centric longitudinal studies: (1) retrospective nature, (2) the use of few recording sessions over time (mostly a baseline and a 1-year follow up) subjected to the confounding effect of disease onset and trajectories in aMCI patients, (3) the lack of a careful characterization of aMCI due to AD as cognitive profile (only one test of episodic memory) and positivity to standard diagnostic biomarkers of AD, and (4) the absence of a control group of aMCI patients not due

to AD with expected different disease evolution over time. The European, prospective, multi-centric study entitled "PharmaCog - E-ADNI" (http://www.pharmacog.org) addressed such limitations. In the PharmaCog study, 147 aMCI patients were screened as APOE genotyping and AD diagnostic markers of CSF and followed longitudinally with clinical, neuropsychological, MRI, rsEEG/ERP, and blood markers for 24 months. The aMCI patients were separated into two sub-groups, namely those "positive" (i.e. prodromal AD) and "negative" to CSF diagnostic markers of AD (i.e. statistical thresholds for Aβ1-42/P-tau ratio based on APOEε4 carrier status [49]). Preparatory PharmaCog studies described the successful multisite MRI harmonization efforts [37–42] and the characterization of the "positive" and "negative" aMCI subjects as neuropsychological, MRI (i.e., hippocampal atrophy, morphometry, and diffusion), and rsEEG/ERP at the baseline stage [6,43,44].

This article is part of a Mini Forum on PharmaCog matrix of biomarkers of prodromal AD in patients with aMCI, which is based on four papers published in Journal of Alzheimer's disease. The specific aim of this article is to evaluate longitudinal functional topographical biomarkers derived from rsfMRI and rsEEG/ERP data in a population of aMCI enrolled in the PharmaCog project and test if these markers can differentiate the group of the "positive" aMCI patients with prodromal AD from the "negative" aMCI subgroup during a time window of 24 months with 5 serial recordings 6 months apart. A linear mixed model adjusted by nuisance covariates was used to investigate those functional biomarkers in terms of Group ("positive" vs "negative" differences regardless of time), Time (temporal effects regardless of Group effects), and Time x Group fixed effects (differential progression between the two subgroups). In the experimental design, the observation time (i.e., 24 months) was expected to account for possible different disease stages in the "positive" and "negative" aMCI patients, while the "negative" aMCI patients were used as a control subgroup. This allowed dissociating, at least in part, cognitive impairment and functional biomarker differences between prodromal and non-prodromal AD in the aMCI subgroups. For sample homogeneity, the statistical design included aMCI data only until conversion to dementia.

2. Materials and Methods

2.1. Participants, clinical exams, and neuropsychological tests

Participants' demographics, clinical, and neuropsychological data have been described in recent PharmaCog studies [6,43,44]. Briefly, 147 aMCI patients were enrolled in 13

European memory clinics of the Innovative Medicine Initiative (IMI) PharmaCog project (http://www.pharmacog.org). Follow-up examinations were performed every 6 months for at least 2 years or until patient progressed to clinical dementia. The main inclusion/exclusion criteria were (1) age between 55 and 90 years; (2) complaints of memory loss by the patient, confirmed by a family relative; (3) Mini-Mental State Examination (MMSE) score of 24 and higher; (4) overall Clinical Dementia Rating score of 0.5; (5) score on the logical memory test lower than 1 standard deviation from the age-adjusted mean; (6) 15-item Geriatric Depression Scale score of 5 or lower; and (7) absence of significant other neurologic, systemic or psychiatric illness.

2.2. Functional MRI data

The multi-site 3T rsfMRI acquisition and analysis protocols have been described in recent studies from the PharmaCog project, also demonstrating high test-retest reproducibility across the Consortium with the use of harmonized MRI acquisition protocols [39,40]. Briefly, 13 European clinical sites equipped with 3.0T scanners used a harmonized MRI acquisition protocol that included structural 3D T1 images [39] and resting state echo-planar imaging (EPI) sessions using manufacturer-provided sequences [40]. This resulted in a sample of 882 rsfMRI datasets (147 subjects, 6 sessions per subject).

Standard brain data preprocessing was performed using SPM8 (http://www.fil.ion.ucl.ac.uk/spm) running under Matlab R2012a (The MathWorks, Inc., Natick MA, USA) and code developed in-house [40]. The main focus of the analysis of rsfMRI data was the functional connectivity within the nodes of DMN, which is expected to be reduced in the early stages of AD [6–8,12,13]. In this line, DMN nodes of interest for this study were the following: medial prefrontal cortex (MFC), bilateral precuneus and posterior cingulate cortex (PCC), and inferior left and right parietal cortex (LPC and RPC, respectively). We also included the left attention frontal-parietal (LFP) network given its potential role in memory cognitive reserve [6,45]. The anatomical characteristics of the DMN and LFP regions and the data analysis procedure are reported in previous methodological study of the Consortium [40]. In brief, Group Independent component analysis (ICA) was performed using 10 spatial components on the concatenated data from each MRI site followed by back-reconstruction [46] to derive the single session DMN and attention LFP network from each subject [40]. DMN regions-of-interest (ROIs) for functional connectivity measurements were obtained by thresholding at $z > 4$ the aggregate DMN site component [40]. For each participant and session, this analysis yielded the average connectivity z-score

within the whole DMN, LFP, and also considering separately each one of the separate nodes within the DMN (PCC, LPC, RPC, and MFC) [40]. These z-scores were used as functional connectivity measures and were the rsfMRI dependent variables in the statistical analyses.

The statistical analyses considered also two MRI-related nuisance regressors for each session, the white matter temporal signal-to-noise ratio (tSNR), given its high variability across sites mostly driven by hardware differences [40], and the median head movement.

2.3. EEG data

Recordings of rsEEG (eyes-closed and -open; N = 126) and auditory "oddball" ERPs (N = 125) were performed by commercial digital EEG systems in the Clinical Units of the PharmaCog Consortium (see more details in [43]). A minimum of 19 scalp electrodes was positioned according to the international 10–20 montage system and referenced to linked earlobes or cephalic reference according to the constraints of the local EEG systems. Ground electrode was placed over the scalp, according to the local standard of the Clinical Units. To monitor eye movements and blinking, bipolar vertical and horizontal electrooculograms (EOGs; 0.3-70 Hz bandpass) were simultaneously recorded. Furthermore, a standard electrocardiographic (EKG) channel was also recorded by a monopolar V6 derivation to remove possible EKG artifacts from EEG data. All electrophysiological data were digitized in continuous recording mode (from 128 to 1000 Hz sampling rate according to the constraints of the local EEG systems). To minimize drowsiness and sleep onset, the duration of the rsEEG recordings was established subject-by-subject from at least 3 minutes to a maximum 5 minutes for each condition (i.e., eyes closed, eyes open).

The rsEEG and ERP data were segmented and analyzed offline in consecutive 2-s and 3-s epochs, respectively. Artifactual epochs were identified using a computerized home-made automatic software procedure [47], confirmed by two EEG experts (CDP, RL), and then eliminated. Artefact-free rsEEG epochs recorded during eyes open condition were used to control the expected reactivity of alpha rhythms as a sign of good quality of rsEEG recordings. Artifact-free rsEEG epochs recorded during eyes open condition were used as an input for the analysis of EEG power density spectrum and cortical source estimation. Concerning ERPs, artifact-free ERP epochs related to frequent and rare stimuli were averaged separately to form individual ERPs for those two classes of auditory stimuli. The latency of the posterior P3b peak following rare stimuli was measured at the Pz electrode and used as a latency reference for further analysis. Based on that latency peak, voltage amplitude was measured at all scalp electrodes in both ERPs related to rare stimuli and those related to

frequent stimuli. For ERP source estimation, individual P3b peak potential distribution was computed according to a standard procedure as the subtraction of P3b peak voltage for the rare stimuli minus the potential distribution for the frequent stimuli at the same latency.

Official exact low-resolution brain electromagnetic tomography (eLORETA) freeware [48] was used for the estimation of cortical sources of the rsEEG and P3b peak data in a standard brain atlas [48]. The following rsEEG/P3b peak markers were estimated: (1) activity of global and regional (i.e. frontal, central, parietal, occipital, temporal, and limbic lobes as defined in the eLORETA brain atlas [48]) normalized cortical (eLORETA) sources of rsEEG rhythms for delta (2-4 Hz), theta (4-7 Hz), alpha 1 (8-10.5 Hz), delta/alpha 1, and theta/alpha 1 bands, as indexes of cortical neural synchronization; and (2) activity of cortical sources of posterior parietal (i.e., Brodmann areas 5, 7, 39, and 40) and posterior cingulate (Brodmann areas 31 and 23) regions generating P3b peak voltage, as an index of cortical neural synchronization related to attention and short-term auditory episodic memory.

2.4. Patients' classification in prodromal AD and control aMCI patients

As mentioned in the Introduction section, the aMCI patients were classified into two subgroups named "positive" (i.e., prodromal AD) and "negative" aMCI based on the results of a Mixture Linear Model with the p sets at < 0.05 [49]. This Model determined the existence of one or more Gaussian populations of aMCI subjects based on the frequency distributions of CSF Aβ42/P-tau levels in the baseline recordings. According to this Model, the aMCI patients were denoted as "positive" aMCI (i.e., prodromal AD) with CSF Aβ42/P-tau levels lower than 15.2 for APOEε4 carriers and 8.9 for APOEε4 non-carriers. The remaining aMCI patients were denoted as "negative" aMCI.

2.5. Statistical analysis

Statistical analyses were performed using SPSS software for descriptive statistics and R software (A language and environment for statistical computing, version 3.4.1) for the computation of Mixture and Linear Mixed Models. Characteristics of the aMCI participants at the baseline recordings were assessed by parametric t-tests (or corresponding non-parametric Mann-Whitney) for continuous Gaussian (or non-Gaussian) distributed variables ($p < 0.05$) and by Chi-square tests for categorical data ($p < 0.05$).

Linear Mixed Models (R-package lme4) were used as statistical tests as they allow the use of individual longitudinal data sets even when some recording sessions are missing in the series (e.g., for technical failures or patients' problems). Specifically, two different types of

Linear Mixed Models were used with all available values of the rsfMRI, rsEEG/P3b peak, and clinical variables in the whole aMCI cohort. In the Models, the fixed effect Group included the two subgroups of "positive" and "negative" aMCI patients, while the fixed effect Time included the values of rsfMRI, rsEEG/P3b peak, and ADAScog13 for baseline recordings and follow-ups at 6, 12, 18, and 24 months. The aMCI patients eventually progressing to dementia were no more called for subsequent follow ups in order to have a relatively homogeneous sample of data relative to aMCI condition. Random intercept and random slope across the variables were used as random effects in the Models to account for individual differences in the biomarkers and ADAScog13 values at baseline as well as for individual changes of those variables across all aMCI patients over follow-ups. All Models were adjusted for age, sex, and education. The output of the Linear Mixed Models was presented in terms of standardized β coefficient, corresponding P-value and, for the interaction factor only, effect size (pseudo h^2) calculated as ratio of explained variability of interaction effect on total variability of each model.

The first Linear Mixed Models of rsfMRI and EEG biomarkers were conducted with Time, Group, and Time X Group interaction as fixed effects. The rsfMRI biomarkers were adjusted also for median head motion and white matter tSNR. The main interest was focused on functional biomarkers (i.e. rsfMRI, rsEEG/P3b peak) associated with the Group effects (regardless of Time), Time effects (regardless of Group), and the Time X Group interaction (the differential progression of the positive aMCI subgroup relative to the negative aMCI subgroup). Specifically, the Group effect showed functional biomarkers distinguishing the two subgroups of aMCI patients regardless the Time effect, while the Group X Time interaction unveiled those biomarkers characterizing the disease progression over-time in the "positive" aMCI subgroup (i.e., prodromal AD).

The second Linear Mixed Models of rsfMRI and EEG biomarkers tested if those functional biomarkers (independent variable) and Time effects predicted cognitive decline over time in the aMCI subgroups as revealed by ADAS-cog13 scores (dependent variable).

3. Results

3.1. Patients' features

Diagnostic markers of CSF and APOE genotypes were available in 144 out of 147 aMCI patients of the PharmaCog/E-ADNI cohort, thus the final data analyses were performed in

144 patients. The main demographic and clinical characteristics of these 144 aMCI patients are reported in Table 1. All of them underwent rsfMRI acquisitions, while a slightly smaller group underwent to rsEEG/ERP recordings (N = 126 patients). The main demographic and clinical characteristics of them are reported in Table 2. In both Tables, as mentioned above, the aMCI patients were aggregated in subgroups based on the baseline Aβ42, phospho tau (P-tau), and total tau (T-tau) values in the CSF as a function of APOE genotype [49]. Compared with the aMCI patients "negative" to CSF Aβ42/P-tau ratio, the "positive" aMCI patients (i.e., prodromal AD) did not differ in age, gender, and education ($p > 0.05$) but showed worse global cognitive performance ($p < 0.05$). MMSE score took into account that difference in the statistical analyses.

Table 3 reports the number of aMCI patients who converted to AD or other non-AD pathologies during the study. The "negative" aMCI patient group did not present conversions to dementia due to AD within 24 months, but presented 2-3% of conversions to dementia due to non-AD pathologies at 12-month follow up and 4-5% at 24-month follow up. In contrast, the "positive" aMCI patients (i.e., prodromal AD) showed 11% of conversion to dementia due to AD at 12-month follow up, 27-29% at 24-month-follow up, and no conversion to dementia due to non-AD pathologies within 24 months.

Please insert Tables 1, 2, and 3 about here

3.2. rsfMRI connectivity measures of prodromal AD

Table 4 reports the results of a Linear Mixed Model showing the variance explained in rsfMRI connectivity measures (population described in Table 3) by the fixed effects of Group ("positive" vs. "negative" group differences regardless of time), Time (temporal differences regardless of group), and Time X Group interaction (differential progression across groups) in aMCI patients over the observation time (24 months, 5 recording session 6 months apart).

Concerning Group and Time, rsfMRI functional connectivity in both the DMN and PCC showed significant effects ($p<0.05$). Specifically, Time effects in DMN and PCC showed a global reduction of functional connectivity over time regardless of Group (DMN: P-value = 0.01, Std β =-0.1; PCC: P-value = 0.05, Std β = -0.09). Furthermore, both DMN and PCC functional connectivity measures also exhibited a significant Group effect pointing to reduced functional connectivity in the "positive" aMCI subgroup (i.e., prodromal AD) compared with the "negative" aMCI subgroup (DMN: P-value = 0.01, Std β = -0.2; PCC: P-value = 0.001, Std β = -0.3). Figure 1 (upper diagrams) illustrates these Group and Time

effects of functional connectivity in PCC. The plot displays the mean modeled connectivity in the two subgroups of aMCI patients over the 5 recording sessions. The profile of DMN changes is very similar (results not shown). As it can be seen in Fig. 1 for PCC, the functional connectivity decay in the time interval of the study is similar in both subgroups, which is consistent with the finding of no significant Time X Group interactions in DMN and PCC.

Interestingly, only functional connectivity in the LPC node showed a significant Time X Group interaction, indicating an increase of connectivity over time in the "positive" (i.e. prodromal AD) relative to the "negative" aMCI subgroup (P-value = 0.01, Std β = 0.2). Figure 2 (upper diagram) illustrates the mean values of rsfMRI connectivity in LPC in the "positive" (i.e., prodromal AD) and "negative" aMCI subgroups over the 5 recording sessions.

The attention LFP network showed no Group effect or Group X Time interaction ($p > 0.05$). Indeed, the only significant finding was a Time effect indicating a lower functional connectivity over time in the LFP network in both "positive" and "negative" aMCI subgroups (P-value = 0.01, Std β = -0.1).

Please insert Table 4 and Figures 1 and 2 about here

3.3. RsEEG and ERP functional biomarkers of prodromal AD

Table 5 reports the results of a Linear Mixed Model showing the variance explained in rsEEG and ERP measures (i.e. functional biomarkers) by the fixed effects of Group ("positive" vs. "negative" aMCI subgroups as defined by CSF Aβ42/P-tau ratio), Time, and Time X Group interaction in aMCI patients over the observation time (24 months, 5 recording sessions 6 months apart). The main interest was focused on the significant Group and Time X Group interaction effects ($p < 0.05$).

Concerning the significant Group effect, 13 rsEEG biomarkers showed higher cortical source activation in the "positive" (i.e., prodromal AD) over the "negative" aMCI subgroup ($p < 0.05$) for frequency bands and ratios (e.g. delta, theta, delta/alpha1, and theta/alpha1) typically associated with abnormally high values in AD patients. The strongest statistical effects were found on global cortical sources of delta rsEEG rhythms (P-value = 0.005, Std β = 0.3) and limbic cortical sources of theta rsEEG rhythms (P-value = 0.004, Std β = 0.3). In the same line, two auditory "oddball" ERP biomarkers also pointed to significant Group effects (e.g., P3b peak as difference between ERPs associated with rare minus frequent

stimuli). Compared to the "negative" aMCI subgroup, the "positive" aMCI subgroup (i.e. prodromal AD) pointed to lower cortical source activation of P3b peak in posterior parietal (P-value = 0.005, Std β = -0.3) and posterior cingulate (P-value = 0.004, Std β = -0.2) regions. Figure 1 (lower diagrams) illustrates the mean values of global cortical sources of delta rsEEG rhythms and cortical source activation of P3b peak in posterior parietal regions in the two subgroups of aMCI patients over the 5 recording sessions.

Concerning the Time X Group interaction (differential progression between "positive" and "negative" subgroups of aMCI patients), only limbic sources of theta rsEEG rhythms showed a significant effect (P-value = 0.046, Std β = 0.1). Results pointed to a *differential* increase of activation in limbic sources of theta rhythms over time in the "positive" (i.e., prodromal AD) compared to the "negative" aMCI subgroup ($p < 0.05$). Figure 2 (bottom) depicts the mean (± SEM) values of those sources in the two subgroups of aMCI patients over the 5 recording sessions.

Please insert Table 5

3.4. Correlation of rsfMRI and EEG markers with ADAS-cog13 score

Linear Mixed Models were also used to test the correlation of rsfMRI and rsEEG/ERP functional biomarkers with ADAS-cog13 scores in the whole aMCI group (all CSF Aβ42/P-tau "positive" and "negative" aMCI patients) and only "positive" aMCI patients (i.e., prodromal AD). As expected, regardless the kind of the functional biomarkers, the Time effect explained an increase of ADAS-cog13 scores (i.e., sign of reduced cognitive performance) in the whole group of aMCI patients over the observation time ($p < 0.001$).

For rsfMRI biomarkers, the increase of ADAS-cog13 score was significantly correlated with a reduction of functional connectivity measured in DMN ($p<0.003$, whole aMCI group; $p<0.002$, CSF Aβ42/P-tau "positive" aMCI subgroup), PCC ($p<0.004$, whole aMCI group; $p<0.003$, CSF Aβ42/P-tau "positive" aMCI subgroup), and LFP network ($p<0.032$, CSF Aβ42/P-tau "positive" aMCI subgroup).

For rsEEG-ERP biomarkers, the increase of ADAS-cog13 score was significantly correlated with an increased activation of occipital sources of theta/alpha 1 rsEEG rhythms in

the “positive” aMCI subgroup (i.e., prodromal AD; $p = 0.041$), these rhythms being typically augmented in magnitude in AD patients.

As a control analysis, Linear Mixed Models were used for the study of the correlation between rsEEG/ERP functional biomarkers and ADAScog13 score in all aMCI patients without the random intercept and random slope as random effects. The Linear Mixed Models were adjusted for age, sex, and education. Results showed that many rsEEG (e.g. central delta, limbic delta, global delta, limbic theta, global theta, frontal theta/alpha 1, central theta/alpha 1, temporal theta/alpha 1, limbic theta/alpha 1, and occipital theta/alpha 1) and ERP (e.g. parietal and posterior cingulate cortex) functional biomarkers pointed to a significant correlation with ADAS-cog13 score measured over the 5 recording sessions ($p < 0.001$). This control finding remarks the substantial impact of the use of random intercept and random slope as random effects in the present Linear Mixed Models. Therefore, the results of the present study are true under the assumption that the factors Group and Time are the fixed effects (independent variables of the statistical design) and the random intercept and random slope of the variables as random effects.

4. Discussion

Functional topographic biomarkers are of interest because they may reflect early interactions between neuropathological alterations specific to prodromal AD (e.g. extracellular accumulation of Aβ1-42 and intracellular aggregation of P-tau in the brain) and the neurophysiological mechanisms of functional brain connectivity and cortical synchronization as measured by rsfMRI and EEG biomarkers, respectively. In the present longitudinal PharmaCog study, we evaluated rsfMRI and rsEEG/ERP functional topographic biomarkers to differentiate a “positive” aMCI (prodromal AD) subgroup relative to a “negative” aMCI subgroup over 24 months.

The two aMCI subgroups were defined according to a standard diagnostic marker of AD in CSF samples (Aβ42/P-tau ratio; [1]), based on the results of a Linear Mixture Model [49]. As expected, a substantial percentage of the “positive” aMCI patients (i.e., prodromal AD) of the present study showed APOEε4 carriers (63%) in line with previous large studies in AD patients [50]. Furthermore, those patients showed a standard annual conversion rate to AD dementia of about 15%, compatible with the use of 1 SD as a threshold of memory deficits in the present inclusion criteria [51]. As another confirmation of the different nature

of aMCI condition in the two subgroups of aMCI patients, none of the "negative" aMCI patients converted to AD dementia within 24 months.

In the present study, functional rsfMRI and EEG topographic biomarkers of prodromal AD were tested by Linear Mixed Models of Group, Time, and Time X Group effects adjusted for nuisance covariates such as age, sex, and education. The models accounted for confounding effects of different disease stages among aMCI patients by using random intercept and slope across the variables of interest and subjects. In what follows, we discuss the main effects of Group ("positive" vs "negative" aMCI subgroup differences regardless of Time) and Time X Group (differential progression profiles across subgroups) on the functional biomarkers evaluated.

Functional biomarkers Group effects

The Linear Mixed Models showed a fixed effect of Group ("positive" versus "negative" aMCI subgroups) on both rsfMRI and EEG (i.e., rsEEG and auditory "oddball" ERPs) topographic biomarkers regardless of Time effects. From a general neurophysiological point of view, this finding suggests that the prodromal AD group can be differentiated from the non-prodromal aMCI group by intrinsic functional connectivity and cortical neural synchronization differences (i.e., at rest), as well as by synchronization differences during the oddball task.

Concerning rsfMRI topographic biomarkers, functional connectivity within the DMN, especially within the PCC, was significantly lower in the "positive" (i.e., prodromal AD) than in the "negative" aMCI subgroup regardless of Time effects, while no group difference was observed in the attention LFP network. This finding complements and extends to the prodromal AD condition a large body of previous rsfMRI evidence of cross-sectional studies pointing to a selective disruption of functional connectivity in DMN regions as possible early functional consequences of amyloid-neurodegenerative cascade on cortical systems underpinning resting state condition and low vigilance in AD patients relative to cognitively intact controls ([6,10,52–55]; for review see [11]). As a novelty, the present finding showed a selective disruption of functional connectivity within DMN regions (no difference at an attention frontoparietal network) using a longitudinal study design with several serial recording sessions and a relatively large sample of aMCI patients suffering from prodromal AD (N = 81) compared with control aMCI patients not due to AD. Such a control group made the present finding on prodromal AD independent of patients' cognitive grade (i.e. all

patients suffered from an aMCI condition), while the longitudinal design with variable intercepts as random effects minimized the confound of patients' disease stage in the comparison of the two aMCI subgroups. The present finding has also the robustness of international multicentric studies using harmonized and qualified MRI scanners [40].

On the whole, the design of the present study overcomes the methodological limitations of typical cross-sectional studies comparing biomarkers in cognitively intact subjects and AD patients. Furthermore, it overcomes the methodological limitations of longitudinal studies just based on one follow up (typically after 1 year). On the other hand, some of the methodological limitations of this study have been previously discussed [40]. In particular, the harmonization of the rsfMRI acquisitions across the 3T Consortium resulted in a common acquisition rate of TR = 2.7 s for full brain coverage. Full brain sub-second acquisition protocols [54] are possible with simultaneous multi-slice selection techniques, which are becoming more widely available as product sequences in clinical scanners and maybe preferable in future studies. The use of higher temporal resolution protocols may improve not only the sensitivity and specificity of rsfMRI connectivity estimates but also enable the exploration of advanced markers of cortical network dynamics [57–59].

The rsfMRI and rsEEG recordings of this study were not recorded simultaneous, yet the results from both modalities refer to a very similar patients' psychophysiological condition as induced by instructions to the patients. In both recordings, aMCI patients were invited to keep eyes closed, stay relaxed, not to sleep, and not focus attention on environmental stimuli or specific internal mental contents (i.e., the so-called "wondering" mental state). In this resting state condition, the mentioned Linear Mixed Models showed a fixed effect of Group ("positive" and "negative" aMCI) on several rsEEG biomarkers. Compared with the "negative" aMCI subgroup, the "positive" (i.e., prodromal AD) aMCI subgroup exhibited lower posterior (parietal, occipital, temporal and limbic) source activity of the low-frequency alpha band (8-10.5 Hz) while widespread delta (< 4 Hz) and theta (4-8 Hz) source activity was higher. These results specify in source space and prodromal AD condition a bulk of previous rsEEG evidence showing that AD patients with dementia are characterized by high power in widespread delta and theta rhythms, as well as low power in posterior alpha and/or beta (13-20 Hz) rhythms [15,21,22,36,60–62]. In temporal areas, delta power is also abnormally high in AD patients with dementia in relation to regional hypometabolism and memory deficits [63]. Furthermore, a short-term cholinergic regimen with Acetylcholinesterase inhibitors partially normalizes theta [64], alpha [65], and delta [66]

rhythms. In the same line, long-term administration of the drug regimen shows beneficial effects on theta and alpha/theta band ratio, especially over the frontal areas [67,68].

Here the Linear Mixed Models also showed a fixed effect of Group ("positive" and "negative" aMCI) on P3b peak of an auditory "oddball" paradigm, namely a typical cognitive task in which patients receive a sequence of frequent (80% of probability) and rare (20%) stimuli with the request to respond with a hand movement or silent counting only to the rare ones (see [69] for a review). In this paradigm, ignoring frequent stimuli and reacting to rare stimuli involves attention and short-term episodic memory. Compared with the "negative" aMCI subgroup, the "positive" (i.e., prodromal AD) aMCI subgroup pointed to lower parietal and posterior cingulate source activities. These findings extend to spatial source localization previous evidence showing that P3b peak amplitude at scalp posterior electrodes was smaller in AD patients than control seniors, as a possible dynamic neural underpinning of abnormal attention and short-term episodic memory information processes. However, these findings did not replicate in the two aMCI subgroups previous slowing of P3b peak latency in aMCI and AD patients with dementia compared with elderly control subjects, even across various "oddball" task difficulties and stimulus modalities [28,70,71]. Those effects were previously discussed as related to AD pathology for visual and olfactory modalities [72,73]. In contrast, the present findings would suggest that P3b peak latency may preferably reflect physiological aging [74] and general deterioration of cognitive performance across pathological aging rather than specific processes of prodromal AD.

Functional biomarkers Time x Group effects: differential progression profiles

Here the Linear Mixed Models showed a significant interaction between Time (5 recording sessions 6 months apart) and Group ("positive" and "negative" aMCI) on both rsfMRI and rsEEG biomarkers. This interaction suggests that in an aMCI group, differential progression profiles between prodromal and non-prodromal AD may be captured by intrinsic functional connectivity (e.g., rsfMRI biomarkers) and cortical neural synchronization (e.g., rsEEG biomarkers).

Concerning rsfMRI biomarkers, we found that the sensitivity to disease progression in aMCI patients varies across cortical networks. Specifically, we found that functional connectivity in the whole DMN, PCC, and LFP were sensitive to short-term longitudinal decay both in the "positive" prodromal AD and the "negative" (control) aMCI patients. But these networks showed no significant differences in the progression of the connectivity

profiles. Instead, functional connectivity in LPC exhibited significant differential effects, with increased functional connectivity over time faster in the “positive” (i.e., prodromal AD) relative to the “negative” aMCI subgroup. Again, this finding stressed the selective feature of this disruption of functional connectivity within DMN regions as compared to the lack of effects in the attention frontoparietal network.

Our longitudinal rsfMRI findings are in good agreement with previous evidence showing both cortical network impairment (connectivity reduction) and compensation (connectivity increase) effects in the DMN in aMCI subjects relative to control seniors, despite gray matter atrophy [7,75–77]. Here we extend those results by confirming similar effects in prodromal AD relative to control aMCI subgroup. Further, the present findings showed a maximum sensitivity of rsfMRI LPC functional connectivity at 2-year follow up, generally consistent with previous longitudinal rsfMRI studies considering baseline and 2-3 year follow-up evaluations in groups of patients with AD dementia and aMCI [7,8,12,77], the latter sometimes diagnosed only on clinical basis. Interestingly, the present lateralization in the left LPC of the effects of longitudinal disease progression in prodromal AD extends recent findings of a longitudinal rsfMRI study with two measurements 2 years apart in a small population of aMCI patients [76]. Such previous study exhibited sensitivity of functional connectivity between left precuneus and other DMN nodes in accounting for the greater progression of aMCI patients in the group of converters to dementia (N=14) than that of non-converters (N=17) [76]. Another recent longitudinal rsfMRI study (baseline and 35 month follow up) in aMCI patients evaluated genotype-by-diagnosis interaction effects [6,78]. Using seed-based rsfMRI analyses on the hippocampus, the Authors detected functional cortical connectivity reductions in APOEε4 carriers and functional cortical connectivity increases in non-carriers. In the light of those findings, the present results should not be interpreted as an indication that rsfMRI functional biomarkers of prodromal AD are limited to DMN nodes. It is reasonable that functional connectivity within the episodic memory brain networks including prefrontal, entorhinal regions, and hippocampus may represent another sensitive dimension in prodromal AD.

Concerning rsEEG biomarkers, the “positive” (i.e., prodromal AD) aMCI subgroup was characterized by increasing limbic source activity of theta rhythms over time. The effect was evident across the serial recordings and robust effects were evident for the progression of prodromal AD in periods of about 12 months. Taking into account the relatively low spatial resolution of the EEG techniques used in the present study (i.e. they cannot disentangle the various limbic regions of cortical midline and medial temporal lobe), this finding suggests a

limbic localization of prodromal AD processes affecting the generation of abnormal rsEEG rhythms during the disease progression in aMCI patients. This topographical suggestion is in line with the well-known localization of initial AD physiopathological processes in entorhinal regions, medial temporal lobe, and midline regions of DMN. Furthermore, it provides a neuroanatomical framework to previous rsEEG evidence showing that AD patients with dementia are characterized by high power in widespread scalp regions of delta and theta rhythms, as well as low power in posterior alpha and/or beta (13-20 Hz) rhythms [17,18,22,79,80].

What do rsfMRI and EEG topographic biomarkers tell us about prodromal AD?

The rsfMRI findings of the present study support the general view that at least for two years, prodromal AD is associated with a partial functional cortical disconnection within DMN nodes in the resting state condition. It can be speculated that this functional disconnection might induce an abnormal elaboration of information about self-body milieu and autobiographical memory, thus affecting the sense of self-awareness and continuity of self across time [6,77]. This speculation is based on the well-known concept that midline cortical nodes of DMN such as PCC and MPF contribute to the integration of the general functions related to the sense of self-awareness [82,83]. In this line of reasoning, PCC might represent information concerning individual's own self-beliefs and first-person perspective in adults [84]. Furthermore, structural maturation of the neural connectivity between PCC and MPF in the adolescence accompanies the development of self-related and social-cognitive functions [85]. Moreover, previous evidence has shown that posterior parietal regions of DMN might contribute to the formation of self-related cognitive representation as a convergence zone binding cortical neural populations involved in the memorization of intermodal details of episodic events concerning the self [86]. Patients with lesions in those parietal regions manifest difficulties in re-experiencing a past autobiographic event when request by experimenters [87]. This speculation encourages the inclusion of cognitive tests probing the richness of the autobiographic memories and self-awareness in prodromal AD patients over time and the analysis with Linear Mixed Models of the correlation between rsfMRI topographic biomarkers of DMN and the performance to those tests.

The rsEEG findings of the present study enlightened neurophysiological mechanisms characterizing prodromal AD patients compared to control aMCI patients. Based on those findings and prior knowledge on the role of thalamocortical loops in the generation of rsEEG

rhythms in humans, it can be speculated that in quiet wakefulness, the abnormal delta and theta source activity in prodromal AD is due to an abnormal interaction between thalamic and cortical pyramidal neural populations, associated with a loss of functional connectivity and a sort of functional isolation of parietal, temporal, and occipital cortical modules [88–90]. It can be also speculated that the alteration of this neurophysiological mechanism is responsible for the reduced parietal and posterior cingulate source activity of auditory "oddball" P3b peak in prodromal AD patients enrolled in the present study. Indeed, P3b peak is mostly an expression of cognitive event-related oscillatory response of thalamocortical circuits oscillating at delta and theta frequencies. In this line, previous studies have shown that delta event-related impulse oscillations in response to visual and auditory "oddball" stimuli were attenuated in amplitude in AD patients with dementia compared with control seniors (see for a review [91]). In AD patients with dementia, an abnormal thalamocortical interaction might be due to a cortical blood hypoperfusion and synaptic dysfunction [63,92–99]. Another cause of such an abnormal thalamocortical interaction might be an impairment of the cortical gray matter especially in the posterior regions [19,30,100–106], as well as a lesion in the brain white matter connecting cerebral cortex [2,6].

Another interesting finding of the present study is the characterization of prodromal AD patients by widespread alpha sources. A tentative neurophysiological explanation of that finding can be based on the insightful research in cats and mice of the group by Dr. Crunelli at Cardiff University. Based on their research, it can be speculated that the reduction of alpha sources in prodromal AD patients over aMCI control patients might denote a progressive alteration in the interplay of glutamatergic and cholinergic neurons, thalamocortical high-threshold, GABAergic interneurons, thalamocortical relay-mode, and cortical pyramidal neurons that constitute the complex network regulating the cortical arousal and vigilance in quiet wakefulness in mammalians [107–109]. In physiological conditions, this network produces cycles of excitation and inhibition in thalamic and cortical neurons that might frame perceptual events in discrete snapshots of approximately 70–100 ms during vigilance [107–109].

Conclusions

In the PharmaCog project, auditory "oddball" ERPs, rsEEG, and rsfMRI functional biomarkers were tested in aMCI patients to characterize prodromal AD. The prodromal AD in patients with aMCI was established based on abnormal CSF levels of amyloid and P-tau

measured at baseline. To take into account the confounding effect of different disease stages and cognitive grades, we used 5 serial recording sessions over 2 years, controlling of cognitive grade using a control group of aMCI patients supposed not due to AD. Functional biomarkers were able to detect significant Group effects stable over time in the prodromal AD patients compared with the control aMCI subgroup: (1) reduced rsfMRI functional connectivity in the DMN and in the PCC node; (2) increased rsEEG source activity at delta (< 4 Hz) and theta (4-8 Hz) rhythms and decreased source activity at alpha (8-10.5 Hz) rhythms; and (3) reduced parietal and posterior cingulate source activities of P3b peak of ERPs. Functional biomarkers were also able to show Time X Group effects, giving differential progression profiles over time in the prodromal AD subgroup relative to the control aMCI subgroup: (1) increased rsfMRI functional connectivity in the LPC node of the DMN and (2) increased limbic source activity at theta rhythms. Topographical biomarkers may have different sensitivity at different phases of the disease [1,110]. At the present stage, we do not know the neuropathological correlates explaining why some rsfMRI and EEG biomarkers were found to be sensitive to Group effects and others to Group X Time effects over 24 months. Future studies correlating those biomarkers with PET maps of Aβ1-42 and P-tau accumulation in the brain may enlighten such an explanation. The effects observed in this study may be related to the progression of the neurodegeneration shown by (1) FDG-PET maps of hypometabolism in parietal and medial temporal cortical areas, (2) atrophy of hippocampus, entorhinal, and temporal neocortex, and (3) biomarkers of tau aggregation in the brain as revealed by CSF samples and PET maps.

The present findings represent the first longitudinal characterization of functional topographic biomarkers of prodromal AD. If cross-validated, these findings may be used for the stratification and monitoring of the effects of disease-modifying drugs in aMCI patients suffering from AD. Indeed, topographic biomarkers of brain function as those derived from rsfMRI and EEG (or the magnetoencephalographic counterpart) may be more likely to respond to an effective disease-modifying intervention relative to structural neuroimaging atrophy markers (e.g., cortical or hippocampus atrophy) or topographic biomarkers of brain hypometabolism (e.g., those measured by FDG-PET), which may only partially recover as they are markedly dependent on neurodegeneration [1].

5. Acknowledgements

This study has been carried out in the Work Package 5 of PharmaCog project (2010-2015, Grant no. 115009; http://www.pharmacog.org). The PharmaCog project was funded by the

Innovative Medicine Initiative of European seventh framework programme, which was granted by European Committee (50%) and European Federation of Pharmaceutical Industries and Associations (50%).

Dr. Giovanni Frisoni's group was supported for the development of this study and extraction of magnetic resonance image (MRI) biomarkers by an in-kind contribution of AstraZeneca AB, Södertälje, Sweden.

Dr. Claudio Babiloni's group was also supported for the extraction of electroencephalographic (EEG) biomarkers by an in-kind contribution of F. Hoffmann-La Roche, Basel, Switzerland.

The Authors are grateful to all members and collaborators of the PharmaCog project and to all amnesic mild cognitive impairment (aMCI) patients who agreed to participate in this study.

6. References

[1] Dubois B, Feldman HH, Jacova C, Hampel H, Molinuevo JL, Blennow K, DeKosky ST, Gauthier S, Selkoe D, Bateman R, Cappa S, Crutch S, Engelborghs S, Frisoni GB, Fox NC, Galasko D, Habert MO, Jicha GA, Nordberg A, Pasquier F, Rabinovici G, Robert P, Rowe C, Salloway S, Sarazin M, Epelbaum S, de Souza LC, Vellas B, Visser PJ, Schneider L, Stern Y, Scheltens P, Cummings JL (2014) Advancing research diagnostic criteria for Alzheimer's disease: the IWG-2 criteria. *Lancet Neurol* **13**, 614–629.

[2] Agosta F, Scola E, Canu E, Marcone A, Magnani G, Sarro L, Copetti M, Caso F, Cerami C, Comi G, Cappa SF, Falini A, Filippi M (2012) White matter damage in frontotemporal lobar degeneration spectrum. *Cereb Cortex* **22**, 2705–2714.

[3] Biswal B, Yetkin FZ, Haughton VM, Hyde JS (1995) Functional connectivity in the motor cortex of resting human brain using echo-planar MRI. *Magn Reson Med* **34**, 537–541.

[4] Fox MD, Raichle ME (2007) Spontaneous fluctuations in brain activity observed with functional magnetic resonance imaging. *Nat Rev Neurosci* **8**, 700–711.

[5] Raichle ME (2015) The brain's default mode network. *Annu Rev Neurosci* **38**, 433–447.

[6] Agosta F, Dalla Libera D, Spinelli EG, Finardi A, Canu E, Bergami A, Bocchio Chiavetto L, Baronio M, Comi G, Martino G, Matteoli M, Magnani G, Verderio C, Furlan R (2014) Myeloid microvesicles in cerebrospinal fluid are associated with myelin damage and neuronal loss in mild cognitive impairment and Alzheimer disease. *Ann Neurol* **76**, 813–825.

[7] Damoiseaux JS (2012) Resting-state fMRI as a biomarker for Alzheimer's disease? *Alzheimers Res Ther* **4**, 8.

[8] Damoiseaux JS, Prater KE, Miller BL, Greicius MD (2012) Functional connectivity tracks clinical deterioration in Alzheimer's disease. *Neurobiol Aging* **33**, 828 e19-30.

[9] Teipel S, Grothe MJ, Zhou J, Sepulcre J, Dyrba M, Sorg C, Babiloni C (2016) Measuring Cortical Connectivity in Alzheimer's Disease as a Brain Neural Network Pathology: Toward Clinical Applications. *J Int Neuropsychol Soc* **22**, 138–163.

[10] Zhang HY, Wang SJ, Liu B, Ma ZL, Yang M, Zhang ZJ, Teng GJ (2010) Resting brain connectivity: changes during the progress of Alzheimer disease. *Radiology* **256**, 598–606.

[11] Zhou J, Liu S, Ng KK, Wang J (2017) Applications of Resting-State Functional Connectivity to Neurodegenerative Disease. *Neuroimaging Clin N Am* **27**, 663–683.

[12] Binnewijzend MA, Schoonheim MM, Sanz-Arigita E, Wink AM, van der Flier WM, Tolboom N, Adriaanse SM, Damoiseaux JS, Scheltens P, van Berckel BN, Barkhof F (2012) Resting-state fMRI changes in Alzheimer's disease and mild cognitive impairment. *Neurobiol Aging* **33**, 2018–2028.

[13] Dennis EL, Thompson PM (2014) Functional brain connectivity using fMRI in aging and Alzheimer's disease. *Neuropsychol Rev* **24**, 49–62.

[14] Babiloni C, Lizio R, Marzano N, Capotosto P, Soricelli A, Triggiani AI, Cordone S,

Gesualdo L, Del Percio C (2016) Brain neural synchronization and functional coupling in Alzheimer's disease as revealed by resting state EEG rhythms. *Int J Psychophysiol* **103**, 88–102.

[15] Babiloni C, Binetti G, Cassetta E, Dal Forno G, Del Percio C, Ferreri F, Ferri R, Frisoni G, Hirata K, Lanuzza B, Miniussi C, Moretti D V, Nobili F, Rodriguez G, Romani GL, Salinari S, Rossini PM (2006) Sources of cortical rhythms change as a function of cognitive impairment in pathological aging: a multicenter study. *Clin Neurophysiol* **117**, 252–268.

[16] Babiloni C, Cassetta E, Binetti G, Tombini M, Del Percio C, Ferreri F, Ferri R, Frisoni G, Lanuzza B, Nobili F, Parisi L, Rodriguez G, Frigerio L, Gurzi M, Prestia A, Vernieri F, Eusebi F, Rossini PM (2007) Resting EEG sources correlate with attentional span in mild cognitive impairment and Alzheimer's disease. *Eur J Neurosci* **25**, 3742–3757.

[17] Babiloni C, Del Percio C, Lizio R, Marzano N, Infarinato F, Soricelli A, Salvatore E, Ferri R, Bonforte C, Tedeschi G, Montella P, Baglieri A, Rodriguez G, Fama F, Nobili F, Vernieri F, Ursini F, Mundi C, Frisoni GB, Rossini PM (2014) Cortical sources of resting state electroencephalographic alpha rhythms deteriorate across time in subjects with amnesic mild cognitive impairment. *Neurobiol Aging* **35**, 130–142.

[18] Babiloni C, Lizio R, Del Percio C, Marzano N, Soricelli A, Salvatore E, Ferri R, Cosentino FI, Tedeschi G, Montella P, Marino S, De Salvo S, Rodriguez G, Nobili F, Vernieri F, Ursini F, Mundi C, Richardson JC, Frisoni GB, Rossini PM (2013) Cortical sources of resting state EEG rhythms are sensitive to the progression of early stage Alzheimer's disease. *J Alzheimers Dis* **34**, 1015–1035.

[19] Babiloni C, Vecchio F, Del Percio C, Montagnese S, Schiff S, Lizio R, Chini G, Serviddio G, Marzano N, Soricelli A, Frisoni GB, Rossini PM, Amodio P (2013) Resting state cortical electroencephalographic rhythms in covert hepatic encephalopathy and Alzheimer's disease. *J Alzheimers Dis* **34**, 707–725.

[20] Babiloni C, Vecchio F, Lizio R, Ferri R, Rodriguez G, Marzano N, Frisoni GB, Rossini PM (2011) Resting state cortical rhythms in mild cognitive impairment and Alzheimer's disease: electroencephalographic evidence. *J Alzheimers Dis* **26 Suppl 3**, 201–214.

[21] Huang C, Wahlund L, Dierks T, Julin P, Winblad B, Jelic V (2000) Discrimination of Alzheimer's disease and mild cognitive impairment by equivalent EEG sources: a cross-sectional and longitudinal study. *Clin Neurophysiol* **111**, 1961–1967.

[22] Jelic V, Johansson SE, Almkvist O, Shigeta M, Julin P, Nordberg A, Winblad B, Wahlund LO (2000) Quantitative electroencephalography in mild cognitive impairment: longitudinal changes and possible prediction of Alzheimer's disease. *Neurobiol Aging* **21**, 533–540.

[23] Koenig T, Prichep L, Dierks T, Hubl D, Wahlund LO, John ER, Jelic V (2005) Decreased EEG synchronization in Alzheimer's disease and mild cognitive impairment. *Neurobiol Aging* **26**, 165–171.

[24] Jervis BW, Belal S, Cassar T, Besleaga M, Bigan C, Michalopoulos K, Zervakis M, Camilleri K, Fabri S (2010) Waveform analysis of non-oscillatory independent components in single-trial auditory event-related activity in healthy subjects and Alzheimer's disease patients. *Curr Alzheimer Res* **7**, 334–347.

[25] Papaliagkas V, Kimiskidis V, Tsolaki M, Anogianakis G (2008) Usefulness of event-related potentials in the assessment of mild cognitive impairment. *BMC Neurosci* **9**, 107.

[26] Papaliagkas VT, Anogianakis G, Tsolaki MN, Koliakos G, Kimiskidis VK (2010) Combination of P300 and CSF beta-amyloid(1-42) assays may provide a potential tool in the early diagnosis of Alzheimer's disease. *Curr Alzheimer Res* **7**, 295–299.

[27] Papaliagkas VT, Kimiskidis VK, Tsolaki MN, Anogianakis G (2011) Cognitive event-related potentials: longitudinal changes in mild cognitive impairment. *Clin Neurophysiol* **122**, 1322–1326.

[28] Polich J, Corey-Bloom J (2005) Alzheimer's disease and P300: review and evaluation of task and modality. *Curr Alzheimer Res* **2**, 515–525.

[29] Tsolaki AC, Kosmidou V, Kompatsiaris IY, Papadaniil C, Hadjileontiadis L, Adam A, Tsolaki M (2017) Brain source localization of MMN and P300 ERPs in mild cognitive impairment and Alzheimer's disease: a high-density EEG approach. *Neurobiol Aging* **55**, 190–201.

[30] Babiloni C, Del Percio C, Boccardi M, Lizio R, Lopez S, Carducci F, Marzano N, Soricelli A, Ferri R, Triggiani AI, Prestia A, Salinari S, Rasser PE, Basar E, Fama F, Nobili F, Yener G, Emek-Savas DD, Gesualdo L, Mundi C, Thompson PM, Rossini PM, Frisoni GB (2015) Occipital sources of resting-state alpha rhythms are related to local gray matter density in subjects with amnesic mild cognitive impairment and Alzheimer's disease. *Neurobiol Aging* **36**, 556–570.

[31] Babiloni C, Del Percio C, Caroli A, Salvatore E, Nicolai E, Marzano N, Lizio R, Cavedo E, Landau S, Chen K, Jagust W, Reiman E, Tedeschi G, Montella P, De Stefano M, Gesualdo L, Frisoni GB, Soricelli A (2016) Cortical sources of resting state EEG rhythms are related to brain hypometabolism in subjects with Alzheimer's disease: an EEG-PET study. *Neurobiol Aging* **48**, 122–134.

[32] Babiloni C, Frisoni G, Steriade M, Bresciani L, Binetti G, Del Percio C, Geroldi C, Miniussi C, Nobili F, Rodriguez G, Zappasodi F, Carfagna T, Rossini PM (2006) Frontal white matter volume and delta EEG sources negatively correlate in awake subjects with mild cognitive impairment and Alzheimer's disease. *Clin Neurophysiol* **117**, 1113–1129.

[33] Babiloni C, Pievani M, Vecchio F, Geroldi C, Eusebi F, Fracassi C, Fletcher E, De Carli C, Boccardi M, Rossini PM, Frisoni GB (2009) White-matter lesions along the cholinergic tracts are related to cortical sources of EEG rhythms in amnesic mild cognitive impairment. *Hum Brain Mapp* **30**, 1431–1443.

[34] Czigler B, Csikos D, Hidasi Z, Anna Gaal Z, Csibri E, Kiss E, Salacz P, Molnar M (2008) Quantitative EEG in early Alzheimer's disease patients - power spectrum and complexity features. *Int J Psychophysiol* **68**, 75–80.

[35] Jelles B, Scheltens P, van der Flier WM, Jonkman EJ, da Silva FH, Stam CJ (2008) Global dynamical analysis of the EEG in Alzheimer's disease: frequency-specific changes of functional interactions. *Clin Neurophysiol* **119**, 837–841.

[36] Jeong J (2004) EEG dynamics in patients with Alzheimer's disease. *Clin Neurophysiol* **115**, 1490–1505.

[37] Albi A, Pasternak O, Minati L, Marizzoni M, Bartres-Faz D, Bargallo N, Bosch B,

Rossini PM, Marra C, Muller B, Fiedler U, Wiltfang J, Roccatagliata L, Picco A, Nobili FM, Blin O, Sein J, Ranjeva JP, Didic M, Bombois S, Lopes R, Bordet R, Gros-Dagnac H, Payoux P, Zoccatelli G, Alessandrini F, Beltramello A, Ferretti A, Caulo M, Aiello M, Cavaliere C, Soricelli A, Parnetti L, Tarducci R, Floridi P, Tsolaki M, Constantinidis M, Drevelegas A, Frisoni G, Jovicich J (2017) Free water elimination improves test-retest reproducibility of diffusion tensor imaging indices in the brain: A longitudinal multisite study of healthy elderly subjects. *Hum Brain Mapp* **38**, 12–26.

[38] Jovicich J, Marizzoni M, Bosch B, Bartres-Faz D, Arnold J, Benninghoff J, Wiltfang J, Roccatagliata L, Picco A, Nobili F, Blin O, Bombois S, Lopes R, Bordet R, Chanoine V, Ranjeva JP, Didic M, Gros-Dagnac H, Payoux P, Zoccatelli G, Alessandrini F, Beltramello A, Bargallo N, Ferretti A, Caulo M, Aiello M, Ragucci M, Soricelli A, Salvadori N, Tarducci R, Floridi P, Tsolaki M, Constantinidis M, Drevelegas A, Rossini PM, Marra C, Otto J, Reiss-Zimmermann M, Hoffmann KT, Galluzzi S, Frisoni GB (2014) Multisite longitudinal reliability of tract-based spatial statistics in diffusion tensor imaging of healthy elderly subjects. *Neuroimage* **101**, 390–403.

[39] Jovicich J, Marizzoni M, Sala-Llonch R, Bosch B, Bartres-Faz D, Arnold J, Benninghoff J, Wiltfang J, Roccatagliata L, Nobili F, Hensch T, Trankner A, Schonknecht P, Leroy M, Lopes R, Bordet R, Chanoine V, Ranjeva JP, Didic M, Gros-Dagnac H, Payoux P, Zoccatelli G, Alessandrini F, Beltramello A, Bargallo N, Blin O, Frisoni GB (2013) Brain morphometry reproducibility in multi-center 3T MRI studies: a comparison of cross-sectional and longitudinal segmentations. *Neuroimage* **83**, 472–484.

[40] Jovicich J, Minati L, Marizzoni M, Marchitelli R, Sala-Llonch R, Bartres-Faz D, Arnold J, Benninghoff J, Fiedler U, Roccatagliata L, Picco A, Nobili F, Blin O, Bombois S, Lopes R, Bordet R, Sein J, Ranjeva JP, Didic M, Gros-Dagnac H, Payoux P, Zoccatelli G, Alessandrini F, Beltramello A, Bargallo N, Ferretti A, Caulo M, Aiello M, Cavaliere C, Soricelli A, Parnetti L, Tarducci R, Floridi P, Tsolaki M, Constantinidis M, Drevelegas A, Rossini PM, Marra C, Schonknecht P, Hensch T, Hoffmann KT, Kuijer JP, Visser PJ, Barkhof F, Frisoni GB (2016) Longitudinal reproducibility of default-mode network connectivity in healthy elderly participants: A multicentric resting-state fMRI study. *Neuroimage* **124**, 442–454.

[41] Marchitelli R, Minati L, Marizzoni M, Bosch B, Bartres-Faz D, Muller BW, Wiltfang J, Fiedler U, Roccatagliata L, Picco A, Nobili F, Blin O, Bombois S, Lopes R, Bordet R, Sein J, Ranjeva JP, Didic M, Gros-Dagnac H, Payoux P, Zoccatelli G, Alessandrini F, Beltramello A, Bargallo N, Ferretti A, Caulo M, Aiello M, Cavaliere C, Soricelli A, Parnetti L, Tarducci R, Floridi P, Tsolaki M, Constantinidis M, Drevelegas A, Rossini PM, Marra C, Schonknecht P, Hensch T, Hoffmann KT, Kuijer JP, Visser PJ, Barkhof F, Frisoni GB, Jovicich J (2016) Test-retest reliability of the default mode network in a multi-centric fMRI study of healthy elderly: Effects of data-driven physiological noise correction techniques. *Hum Brain Mapp* **37**, 2114–2132.

[42] Marizzoni M, Antelmi L, Bosch B, Bartres-Faz D, Muller BW, Wiltfang J, Fiedler U, Roccatagliata L, Picco A, Nobili F, Blin O, Bombois S, Lopes R, Sein J, Ranjeva JP, Didic M, Gros-Dagnac H, Payoux P, Zoccatelli G, Alessandrini F, Beltramello A, Bargallo N, Ferretti A, Caulo M, Aiello M, Cavaliere C, Soricelli A, Salvadori N, Parnetti L, Tarducci R, Floridi P, Tsolaki M, Constantinidis M, Drevelegas A, Rossini PM, Marra C, Hoffmann KT, Hensch T, Schonknecht P, Kuijer JP, Visser PJ, Barkhof F, Bordet R, Frisoni GB, Jovicich J (2015) Longitudinal reproducibility of automatically segmented hippocampal subfields: A multisite European 3T study on

healthy elderly. *Hum Brain Mapp* **36**, 3516–3527.

[43] Galluzzi S, Marizzoni M, Babiloni C, Albani D, Antelmi L, Bagnoli C, Bartres-Faz D, Cordone S, Didic M, Farotti L, Fiedler U, Forloni G, Girtler N, Hensch T, Jovicich J, Leeuwis A, Marra C, Molinuevo JL, Nobili F, Pariente J, Parnetti L, Payoux P, Del Percio C, Ranjeva JP, Rolandi E, Rossini PM, Schonknecht P, Soricelli A, Tsolaki M, Visser PJ, Wiltfang J, Richardson JC, Bordet R, Blin O, Frisoni GB (2016) Clinical and biomarker profiling of prodromal Alzheimer's disease in workpackage 5 of the Innovative Medicines Initiative PharmaCog project: a "European ADNI study." *J Intern Med* **279**, 576–591.

[44] Nathan PJ, Lim YY, Abbott R, Galluzzi S, Marizzoni M, Babiloni C, Albani D, Bartres-Faz D, Didic M, Farotti L, Parnetti L, Salvadori N, Muller BW, Forloni G, Girtler N, Hensch T, Jovicich J, Leeuwis A, Marra C, Molinuevo JL, Nobili F, Pariente J, Payoux P, Ranjeva JP, Rolandi E, Rossini PM, Schonknecht P, Soricelli A, Tsolaki M, Visser PJ, Wiltfang J, Richardson JC, Bordet R, Blin O, Frisoni GB (2017) Association between CSF biomarkers, hippocampal volume and cognitive function in patients with amnestic mild cognitive impairment (MCI). *Neurobiol Aging* **53**, 1–10.

[45] Franzmeier N, Gottler J, Grimmer T, Drzezga A, Araque-Caballero MA, Simon-Vermot L, Taylor ANW, Burger K, Catak C, Janowitz D, Muller C, Duering M, Sorg C, Ewers M (2017) Resting-State Connectivity of the Left Frontal Cortex to the Default Mode and Dorsal Attention Network Supports Reserve in Mild Cognitive Impairment. *Front Aging Neurosci* **9**, 264.

[46] Calhoun VD, Adali T, Pearlson GD, Pekar JJ (2001) A method for making group inferences from functional MRI data using independent component analysis. *Hum Brain Mapp* **14**, 140–151.

[47] Moretti D V, Babiloni F, Carducci F, Cincotti F, Remondini E, Rossini PM, Salinari S, Babiloni C (2003) Computerized processing of EEG-EOG-EMG artifacts for multi-centric studies in EEG oscillations and event-related potentials. *Int J Psychophysiol* **47**, 199–216.

[48] Pascual-Marqui (2007) Discrete, 3D distributed, linear imaging methods of electric neuronal activity. Part 1: exact, zero error localization. *Clin Neurophysiol* **112**, 7.

[49] Marizzoni M, Ferrari C, Galluzzi S, Jovicich J, Albani D, Babiloni C, Didic M, Forloni G, Molinuevo JL, Nobili FM, Parnetti L, Payoux P, Rossini PM, Schönknecht P, Soricelli A, Tsolaki M, Visser PJ, Wiltfang J, Bordet R, Cavaliere L, Richardson J, Blin O, Frisoni GB (2017) CSF biomarkers and effect of apolipoprotein E genotype, age and sec on cut-off derivation in mild cognitive impairment. *Alzheimer's Dement.* **13**, P1319.

[50] Geifman N, Brinton RD, Kennedy RE, Schneider LS, Butte AJ (2017) Evidence for benefit of statins to modify cognitive decline and risk in Alzheimer's disease. *Alzheimers. Res. Ther.* **9**, 10.

[51] Amieva H, Letenneur L, Dartigues J-F, Rouch-Leroyer I, Sourgen C, D'Alchee-Biree F, Dib M, Barberger-Gateau P, Orgogozo J-M, Fabrigoule C (2004) Annual rate and predictors of conversion to dementia in subjects presenting mild cognitive impairment criteria defined according to a population-based study. *Dement. Geriatr. Cogn. Disord.* **18**, 87–93.

[52] Gili T, Cercignani M, Serra L, Perri R, Giove F, Maraviglia B, Caltagirone C, Bozzali

M (2011) Regional brain atrophy and functional disconnection across Alzheimer's disease evolution. *J Neurol Neurosurg Psychiatry* **82**, 58–66.

[53] Lau WK, Leung MK, Lee TM, Law AC (2016) Resting-state abnormalities in amnestic mild cognitive impairment: a meta-analysis. *Transl Psychiatry* **6**, e790.

[54] Petrella JR, Sheldon FC, Prince SE, Calhoun VD, Doraiswamy PM (2011) Default mode network connectivity in stable vs progressive mild cognitive impairment. *Neurology* **76**, 511–517.

[55] Song J, Qin W, Liu Y, Duan Y, Liu J, He X, Li K, Zhang X, Jiang T, Yu C (2013) Aberrant functional organization within and between resting-state networks in AD. *PLoS One* **8**, e63727.

[56] Feinberg DA, Moeller S, Smith SM, Auerbach E, Ramanna S, Gunther M, Glasser MF, Miller KL, Ugurbil K, Yacoub E (2010) Multiplexed echo planar imaging for sub-second whole brain FMRI and fast diffusion imaging. *PLoS One* **5**, e15710.

[57] de Pasquale F, Corbetta M, Betti V, Della Penna S (2017) Cortical cores in network dynamics. *Neuroimage*.

[58] Preibisch C, Castrillon GJ, Buhrer M, Riedl V (2015) Evaluation of Multiband EPI Acquisitions for Resting State fMRI. *PLoS One* **10**, e0136961.

[59] Wig GS (2017) Segregated Systems of Human Brain Networks. *Trends Cogn Sci* **21**, 981–996.

[60] Dierks T, Ihl R, Frolich L, Maurer K (1993) Dementia of the Alzheimer type: effects on the spontaneous EEG described by dipole sources. *Psychiatry Res* **50**, 151–162.

[61] Dierks T, Jelic V, Pascual-Marqui RD, Wahlund L, Julin P, Linden DE, Maurer K, Winblad B, Nordberg A (2000) Spatial pattern of cerebral glucose metabolism (PET) correlates with localization of intracerebral EEG-generators in Alzheimer's disease. *Clin Neurophysiol* **111**, 1817–1824.

[62] Ponomareva N V, Selesneva ND, Jarikov GA (2003) EEG alterations in subjects at high familial risk for Alzheimer's disease. *Neuropsychobiology* **48**, 152–159.

[63] Valladares-Neto DC, Buchsbaum MS, Evans WJ, Nguyen D, Nguyen P, Siegel B V, Stanley J, Starr A, Guich S, Rice D (1995) EEG delta, positron emission tomography, and memory deficit in Alzheimer's disease. *Neuropsychobiology* **31**, 173–181.

[64] Brassen S, Adler G (2003) Short-term effects of acetylcholinesterase inhibitor treatment on EEG and memory performance in Alzheimer patients: an open, controlled trial. *Pharmacopsychiatry* **36**, 304–308.

[65] Onofrj M, Thomas A, Iacono D, Luciano AL, Di Iorio A (2003) The effects of a cholinesterase inhibitor are prominent in patients with fluctuating cognition: a part 3 study of the main mechanism of cholinesterase inhibitors in dementia. *Clin Neuropharmacol* **26**, 239–251.

[66] Reeves RR, Struve FA, Patrick G (2002) The effects of donepezil on quantitative EEG in patients with Alzheimer's disease. *Clin Electroencephalogr* **33**, 93–96.

[67] Kogan EA, Korczyn AD, Virchovsky RG, Klimovizky Ss, Treves TA, Neufeld MY (2001) EEG changes during long-term treatment with donepezil in Alzheimer's disease patients. *J Neural Transm* **108**, 1167–1173.

[68] Rodriguez G, Vitali P, De Leo C, De Carli F, Girtler N, Nobili F (2002) Quantitative EEG changes in Alzheimer patients during long-term donepezil therapy. *Neuropsychobiology* **46**, 49–56.

[69] Rossini PM, Rossi S, Babiloni C, Polich J (2007) Clinical neurophysiology of aging brain: from normal aging to neurodegeneration. *Prog Neurobiol* **83**, 375–400.

[70] Golob EJ, Irimajiri R, Starr A (2007) Auditory cortical activity in amnestic mild cognitive impairment: relationship to subtype and conversion to dementia. *Brain* **130**, 740–752.

[71] Polich J, Comerchero MD (2003) P3a from visual stimuli: typicality, task, and topography. *Brain Topogr* **15**, 141–152.

[72] Morgan CD, Murphy C (2002) Olfactory event-related potentials in Alzheimer's disease. *J Int Neuropsychol Soc* **8**, 753–763.

[73] Polich J, Pitzer A (1999) P300 and Alzheimer's disease: oddball task difficulty and modality effects. *Electroencephalogr Clin Neurophysiol Suppl* **50**, 281–287.

[74] van Dinteren R, Arns M, Jongsma MLA, Kessels RPC (2014) P300 development across the lifespan: a systematic review and meta-analysis. *PLoS One* **9**, e87347.

[75] Qi Z, Wu X, Wang Z, Zhang N, Dong H, Yao L, Li K (2010) Impairment and compensation coexist in amnestic MCI default mode network. *Neuroimage* **50**, 48–55.

[76] Serra L, Cercignani M, Mastropasqua C, Torso M, Spano B, Makovac E, Viola V, Giulietti G, Marra C, Caltagirone C, Bozzali M (2016) Longitudinal Changes in Functional Brain Connectivity Predicts Conversion to Alzheimer's Disease. *J Alzheimers Dis* **51**, 377–389.

[77] Bai F, Liao W, Watson DR, Shi Y, Yuan Y, Cohen AD, Xie C, Wang Y, Yue C, Teng Y, Wu D, Jia J, Zhang Z (2011) Mapping the altered patterns of cerebellar resting-state function in longitudinal amnestic mild cognitive impairment patients. *J Alzheimers Dis* **23**, 87–99.

[78] Ye Q, Su F, Shu H, Gong L, Xie CM, Zhou H, Zhang ZJ, Bai F (2017) Shared effects of the clusterin gene on the default mode network among individuals at risk for Alzheimer's disease. *CNS Neurosci Ther* **23**, 395–404.

[79] Coben LA, Danziger W, Storandt M (1985) A longitudinal EEG study of mild senile dementia of Alzheimer type: changes at 1 year and at 2.5 years. *Electroencephalogr Clin Neurophysiol* **61**, 101–112.

[80] Soininen H, Partanen J, Laulumaa V, Helkala EL, Laakso M, Riekkinen PJ (1989) Longitudinal EEG spectral analysis in early stage of Alzheimer's disease. *Electroencephalogr Clin Neurophysiol* **72**, 290–297.

[81] Weiler M, Northoff G, Damasceno BP, Balthazar MLF (2016) Self, cortical midline structures and the resting state: Implications for Alzheimer's disease. *Neurosci Biobehav Rev* **68**, 245–255.

[82] Northoff G, Bermpohl F (2004) Cortical midline structures and the self. *Trends Cogn Sci* **8**, 102–107.

[83] Northoff G, Heinzel A, de Greck M, Bermpohl F, Dobrowolny H, Panksepp J (2006) Self-referential processing in our brain--a meta-analysis of imaging studies on the self.

Neuroimage **31**, 440–457.

[84] Ochsner KN, Beer JS, Robertson ER, Cooper JC, Gabrieli JD, Kihsltrom JF, D'Esposito M (2005) The neural correlates of direct and reflected self-knowledge. *Neuroimage* **28**, 797–814.

[85] Supekar K, Uddin LQ, Prater K, Amin H, Greicius MD, Menon V (2010) Development of functional and structural connectivity within the default mode network in young children. *Neuroimage* **52**, 290–301.

[86] Shimamura AP (2011) Episodic retrieval and the cortical binding of relational activity. *Cogn Affect Behav Neurosci* **11**, 277–291.

[87] Berryhill ME (2012) Insights from neuropsychology: pinpointing the role of the posterior parietal cortex in episodic and working memory. *Front Integr Neurosci* **6**, 31.

[88] Klimesch W (1999) EEG alpha and theta oscillations reflect cognitive and memory performance: a review and analysis. *Brain Res Brain Res Rev* **29**, 169–195.

[89] Pfurtscheller G, Lopes da Silva FH (1999) Event-related EEG/MEG synchronization and desynchronization: basic principles. *Clin Neurophysiol* **110**, 1842–1857.

[90] Steriade M, Llinas RR (1988) The functional states of the thalamus and the associated neuronal interplay. *Physiol Rev* **68**, 649–742.

[91] Yener GG, Basar E (2013) Biomarkers in Alzheimer's disease with a special emphasis on event-related oscillatory responses. *Suppl Clin Neurophysiol* **62**, 237–273.

[92] Rae-Grant A, Blume W, Lau C, Hachinski VC, Fisman M, Merskey H (1987) The electroencephalogram in Alzheimer-type dementia. A sequential study correlating the electroencephalogram with psychometric and quantitative pathologic data. *Arch Neurol* **44**, 50–54.

[93] Brenner RP, Ulrich RF, Spiker DG, Sclabassi RJ, Reynolds 3rd CF, Marin RS, Boller F (1986) Computerized EEG spectral analysis in elderly normal, demented and depressed subjects. *Electroencephalogr Clin Neurophysiol* **64**, 483–492.

[94] Stigsby B, Johannesson G, Ingvar DH (1981) Regional EEG analysis and regional cerebral blood flow in Alzheimer's and Pick's diseases. *Electroencephalogr Clin Neurophysiol* **51**, 537–547.

[95] Kwa VI, Weinstein HC, Posthumus Meyjes EF, van Royen EA, Bour LJ, Verhoeff PN, Ongerboer de Visser BW (1993) Spectral analysis of the EEG and 99m-Tc-HMPAO SPECT-scan in Alzheimer's disease. *Biol Psychiatry* **33**, 100–107.

[96] Niedermeyer E (1997) Alpha rhythms as physiological and abnormal phenomena. *Int J Psychophysiol* **26**, 31–49.

[97] Passero S, Rocchi R, Vatti G, Burgalassi L, Battistini N (1995) Quantitative EEG mapping, regional cerebral blood flow, and neuropsychological function in Alzheimer's disease. *Dementia* **6**, 148–156.

[98] Rodriguez G, Copello F, Vitali P, Perego G, Nobili F (1999) EEG spectral profile to stage Alzheimer's disease. *Clin Neurophysiol* **110**, 1831–1837.

[99] Steriade M (1994) Sleep oscillations and their blockage by activating systems. *J Psychiatry Neurosci* **19**, 354–358.

[100] Killiany RJ, Moss MB, Albert MS, Sandor T, Tieman J, Jolesz F (1993) Temporal lobe regions on magnetic resonance imaging identify patients with early Alzheimer's disease. *Arch Neurol* **50**, 949–954.

[101] Fernandez A, Arrazola J, Maestu F, Amo C, Gil-Gregorio P, Wienbruch C, Ortiz T (2003) Correlations of hippocampal atrophy and focal low-frequency magnetic activity in Alzheimer disease: volumetric MR imaging-magnetoencephalographic study. *AJNR Am J Neuroradiol* **24**, 481–487.

[102] Delli Pizzi S, Maruotti V, Taylor JP, Franciotti R, Caulo M, Tartaro A, Thomas A, Onofrj M, Bonanni L (2014) Relevance of subcortical visual pathways disruption to visual symptoms in dementia with Lewy bodies. *Cortex* **59**, 12–21.

[103] Delli Pizzi S, Franciotti R, Taylor JP, Esposito R, Tartaro A, Thomas A, Onofrj M, Bonanni L (2015) Structural Connectivity is Differently Altered in Dementia with Lewy Body and Alzheimer's Disease. *Front Aging Neurosci* **7**, 208.

[104] Delli Pizzi S, Padulo C, Brancucci A, Bubbico G, Edden RA, Ferretti A, Franciotti R, Manippa V, Marzoli D, Onofrj M, Sepede G, Tartaro A, Tommasi L, Puglisi-Allegra S, Bonanni L (2016) GABA content within the ventromedial prefrontal cortex is related to trait anxiety. *Soc Cogn Affect Neurosci* **11**, 758–766.

[105] Graff-Radford J, Madhavan M, Vemuri P, Rabinstein AA, Cha RH, Mielke MM, Kantarci K, Lowe V, Senjem ML, Gunter JL, Knopman DS, Petersen RC, Jack Jr. CR, Roberts RO (2016) Atrial fibrillation, cognitive impairment, and neuroimaging. *Alzheimers Dement* **12**, 391–398.

[106] Sarro L, Senjem ML, Lundt ES, Przybelski SA, Lesnick TG, Graff-Radford J, Boeve BF, Lowe VJ, Ferman TJ, Knopman DS, Comi G, Filippi M, Petersen RC, Jack Jr. CR, Kantarci K (2016) Amyloid-beta deposition and regional grey matter atrophy rates in dementia with Lewy bodies. *Brain* **139**, 2740–2750.

[107] Hughes SW, Crunelli V (2005) Thalamic mechanisms of EEG alpha rhythms and their pathological implications. *Neuroscientist* **11**, 357–372.

[108] Lorincz ML, Crunelli V, Hughes SW (2008) Cellular dynamics of cholinergically induced alpha (8-13 Hz) rhythms in sensory thalamic nuclei in vitro. *J Neurosci* **28**, 660–671.

[109] Lorincz ML, Kekesi KA, Juhasz G, Crunelli V, Hughes SW (2009) Temporal framing of thalamic relay-mode firing by phasic inhibition during the alpha rhythm. *Neuron* **63**, 683–696.

[110] Frisoni GB, Fox NC, Jack CR, Scheltens P, Thompson PM (2010) The clinical use of structural MRI in Alzheimer disease. *Nat. Rev. Neurol.* **6**, 67–77.

Table legends

Table 1: *Clinical and socio-demographic features of amnesic mild cognitive impairment (aMCI) patients receiving resting state functional magnetic resonance imaging recordings (rsfMRI) in the present study. Patients were stratified into cerebrospinal (CSF) Aβ42/P-tau "positive" and "negative" according to APOE4-specific cut-offs for carriers and non-carriers of APOE4 genotyping. See Methods section for more details.*

	"Negative" aMCI (N = 63)	**"Positive" aMCI** (N = 81)	**P value**[a]
Age, mean (Standard Deviation, SD)	68.3 (8.4)	69.8 (6.3)	.2
Sex, F/M, No.	36/27	46/35	1
Education, mean (SD)	10.0 (4.3)	11.1 (4.4)	.1
APOEε4 carriers, No. (%)	3 (5)	63 (78)	**<.001**
MMSE score, mean (SD)	27.1 (1.8)	26.2 (1.8)	**.006**
ADAS-cog13, mean (SD)[b,c]	19.1 (5.9)	21.6 (8.1)	.052
CSF biomarkers, mean (SD, pg/ml)			
Aβ42	949 (244)	495 (132)	**<.001**
P-Tau	47 (15)	84 (38)	**<.001**
T-tau	301 (149)	614 (394)	**<.001**

[a] Assessed by ANOVA (for continuous Gaussian distributed variables) or Kruskall-Wallis with Dunn correction (for continuous non-Gaussian distributed variables) and Chi-square tests (for categorical variables).

[b] Range 0-85, with 0 as the best score.

[c] Information was missing for 1 patient.

Abbreviations: Legend: MMSE, mini mental state evaluation; SD, standard deviation; ADAS-cog13, Alzheimer Disease Assessment Scale-Cognitive Subscale, version 13; Aβ42, β-amyloid; APOE, apolipoprotein E; CSF, cerebrospinal fluid; P-tau, tau phosphorylated at threonine 181; T-tau, total tau; SD, standard deviation.

Table 2: *Clinical and socio-demographic features of aMCI patients undergone to resting state electroencephalographic (rsEEG) and event-related potential (ERP) recordings in the present study. These patients, a subgroup of those described in Table 1, were stratified into CSF Aβ42/P-tau "positive" and "negative" according to APOE4-specific cut-offs for carriers and non-carriers of APOE4 genotyping. See Methods section for more details.*

	"Negative" aMCI (N = 54)	**"Positive" aMCI** (N = 72)	**P value** [a]
Age, mean (Standard Deviation, SD)	68.5 (8.5)	69.9 (6.0)	.2
Sex, F/M, No.	30/24	42/30	0.8
Education, mean (SD)	9.9 (4.1)	11.0 (4.5)	.2
APOEε4 carriers, No. (%)	3.7%	77.8%	**<.001**
MMSE, mean (SD)	26.3 (2.2)	25.2 (2.2)	**.01**
ADAS-cog13, mean (SD) [b]	20.2 (6.8)	23.1 (7.7)	**.04**
CSF biomarkers, mean (SD, pg/ml)			
Aβ42	932 (253)	500 (132)	**<.001**
P-Tau	47 (15)	84 (36)	**<.001**
T-tau	297 (151)	600 (316)	**<.001**

[a] Assessed by ANOVA (for continuous Gaussian distributed variables) or Kruskal-Wallis with Dunn correction (for continuous non-Gaussian distributed variables) and Chi-square tests (for categorical variables).

[b] Range 0-85, with 0 as the best score.

Abbreviations: ADAS-cog13, Alzheimer Disease Assessment Scale-Cognitive Subscale, version 13; Aβ42, β-amyloid; APOE, Apolipoprotein E; CSF, cerebrospinal fluid; P-tau, tau phosphorylated at threonine 181; T-tau, total tau; SD, standard deviation.

Table 3: *Number of patients who converted from aMCI to dementia due to AD and other pathologies. These patients were stratified into CSF Aβ42/P-tau "positive" and "negative" according to APOE4-specific cut-offs for carriers and non-carriers of APOE4 genotyping. See Methods section for more details.*

aMCI patients with rsfMRI recordings		
	CSF Aβ42/P-tau "negative" aMCI group	**CSF Aβ42/P-tau "positive" aMCI group**
N	63	81
Converted in AD (12 months)	0.0% (N=0)	11.1% (N=9)
Converted in AD (24 months)	0.0% (N=0)	27.2% (N=22)
Converted in other dementias (12 months)	3.2% (N=2)	0.0% (N=0)
Converted in other dementias (24 months)	4.8% (N=3)	0.0% (N=0)
aMCI patients with rsEEG/ERP recordings		
	CSF Aβ42/P-tau "negative" aMCI group	**CSF Aβ42/P-tau "positive" aMCI group**
N	54	72
Converted in AD (12 months)	0.0% (N=0)	11.1% (N=8)
Converted in AD (24 months)	0.0% (N=0)	29.2% (N=21)
Converted in other dementias (12 months)	1.9% (N=1)	0.0% (N=0)
Converted in other dementias (24 months)	3.7% (N=2)	0.0% (N=0)

Table 4: *Resting state fMRI nodes showing significant functional connectivity effects explained by a Linear Mixed Model of longitudinal changes (baseline, 6, 12, 18, 24 months follow ups) in aMCI patients stratified into two groups ("positive" as prodromal AD and "negative" as a control group). The model included Group (Aβ42/P-tau ratio), Time, and Time X Group interaction as main predictors of interest adjusted by age, sex, baseline MMSE score, temporal signal-to-noise ratio, and mean fractional head displacement as nuisance variables. Significant (P-value < 0.05) fixed effects are emphasized in bold. Abbreviations: DMN, default mode network (all nodes); PCC, posterior cingulate cortex; LPC, inferior left parietal cortex; LFP, left attention frontal-parietal network; Std β, standardized β coefficient of Linear Mixed Model.*

rsfMRI connectivity measure	**Group**		**Time**		**Time X Group**	
	Std β	**P-value**	**Std β**	**P-value**	**Std β**	**P-value**
PCC	-0.3	**0.001**	-0.09	**0.04**	-0.05	0.5
LPC	0.2	0.08	-0.06	0.100	0.2	**0.01**
DMN	-0.2	**0.01**	-0.1	**0.01**	0.01	0.9
LFP	-0.002	1	-0.1	**0.01**	0.03	0.8

Table 5: *Resting state EEG and auditory oddball ERP measures showing significant cortical neural synchronization effects explained by a Linear Mixed Model of longitudinal changes (baseline, 6, 12, 18, 24 months follow ups) in aMCI patients stratified into two groups ("positive" as prodromal AD and "negative" as a control group). ERP component of interest was the P3b peak as difference between ERPs peaking about 400 ms post-stimulus associated with rare minus frequent stimuli. The model included Group (Aβ42/P-tau ratio), Time, and Time X Group interaction as main predictors of interest adjusted by age, sex and baseline MMSE score as nuisance variables. Significant (P-value < 0.05) fixed effects are emphasized in bold. Abbreviation: Std β, standardized β coefficient of the Linear Mixed Model.*

rsEEG/ERP measures	Group		Time		Time X Group	
	Std β	P-value	Std β	P-value	Std β	P-value
Central delta rsEEG	0.2	**0.014**	-0.0	0.5	0.1	0.2
Temporal delta rsEEG	0.2	**0.044**	0.0	0.6	0.0	0.5
Limbic delta rsEEG	0.2	**0.031**	0.0	0.3	0.1	0.5
Global delta rsEEG	0.3	**0.005**	0.0	1.0	0.1	0.1
Limbic theta rsEEG	0.3	**0.004**	-0.0	0.6	0.1	**0.046**
Global theta rsEEG	0.2	**0.020**	-0.0	0.6	0.1	0.1
Parietal delta/alpha1 rsEEG	0.2	**0.038**	-0.1	0.2	0.1	0.2
Frontal theta/alpha1 rsEEG	0.2	**0.045**	0.0	0.9	0.1	0.5
Central theta/alpha1 rsEEG	0.3	**0.009**	-0.0	0.6	0.1	0.1
Occipital theta/alpha1 rsEEG	0.2	**0.049**	-0.1	0.1	0.1	0.1

Temporal theta/alpha1 rsEEG	0.2	**0.016**	-0.0	0.3	0.1	0.1
Limbic theta/alpha1 rsEEG	0.3	**0.010**	-0.0	0.8	0.1	0.1
Global theta/alpha1 rsEEG	0.2	**0.013**	-0.0	0.4	0.1	0.1
Parietal P3b peak	-0.3	**0.005**	0.0	0.5	-0.2	0.1
Posterior cingulate P3b peak	-0.2	**0.017**	0.0	0.6	-0.2	0.1

Figure Legends

Figure 1. *Longitudinal profile of functional topographical biomarkers showing significant Group effects regardless of time (p-value < 0.05). Patients were stratified in two amnesic mild cognitive impairment (aMCI) subgroups: Aβ42/P-tau "positive" (red) as prodromal AD as an experimental subgroup and Aβ42/P-tau "negative" (green) as a control subgroup. Mean (± standard error of the mean, SEM) model values are shown from 5 recording sessions starting at time zero (baseline) and 6-, 12-, 18, and 24-month follow-ups. Top: resting state functional magnetic resonance imaging (rsfMRI) functional connectivity measures in the precuneus and posterior cingulate cortex (PCC) of the DMN. Of note, functional rsfMRI connectivity in both PCC and global default mode network (DMN; not shown) gave a similar pattern of significant Group effects (connectivity reduction in "positive" group regardless of time) and Time effects (functional decay in Time regardless of Group, p-value < 0.05). Middle: Mean (± standard error of the mean, SEM) values of global cortical sources of resting state electroencephalographic (rsEEG) rhythms at delta frequency band (< 4 Hz). Bottom: mean (± SEM) values of parietal cortical sources of auditory "oddball" event-related potentials (ERPs) peaking at about 400 ms (P3b peak) post-stimulus following rare minus frequent stimuli in those groups.*

Figure 2. *Longitudinal profile of functional topographical biomarkers showing significant Time x Group effects (p-value < 0.05). Patients were stratified in two aMCI groups: Aβ42/P-tau "positive" (red) as prodromal AD and Aβ42/P-tau "negative" (green) as a control group. Mean (± standard error of the mean, SEM) model values are shown from 5 recording session starting at time zero (baseline) and 6-, 12-, 18, and 24-month follow-ups. Time x Group effects show differential progression in the two groups. Top: rsfMRI functional connectivity measures in the left parietal cortex (LPC) of the DMN, showing a progression towards increased connectivity in the "positive" aMCI subgroup relative to the "negative" aMCI subgroup. Bottom. Mean (± SEM) values of cortical limbic sources of rsEEG rhythms at theta frequency band (4-8 Hz), showing an increase in cortical neural synchronization in the "positive" (i.e., prodromal AD) subgroup relative to the "negative" aMCI control subgroup.*

Figure 1

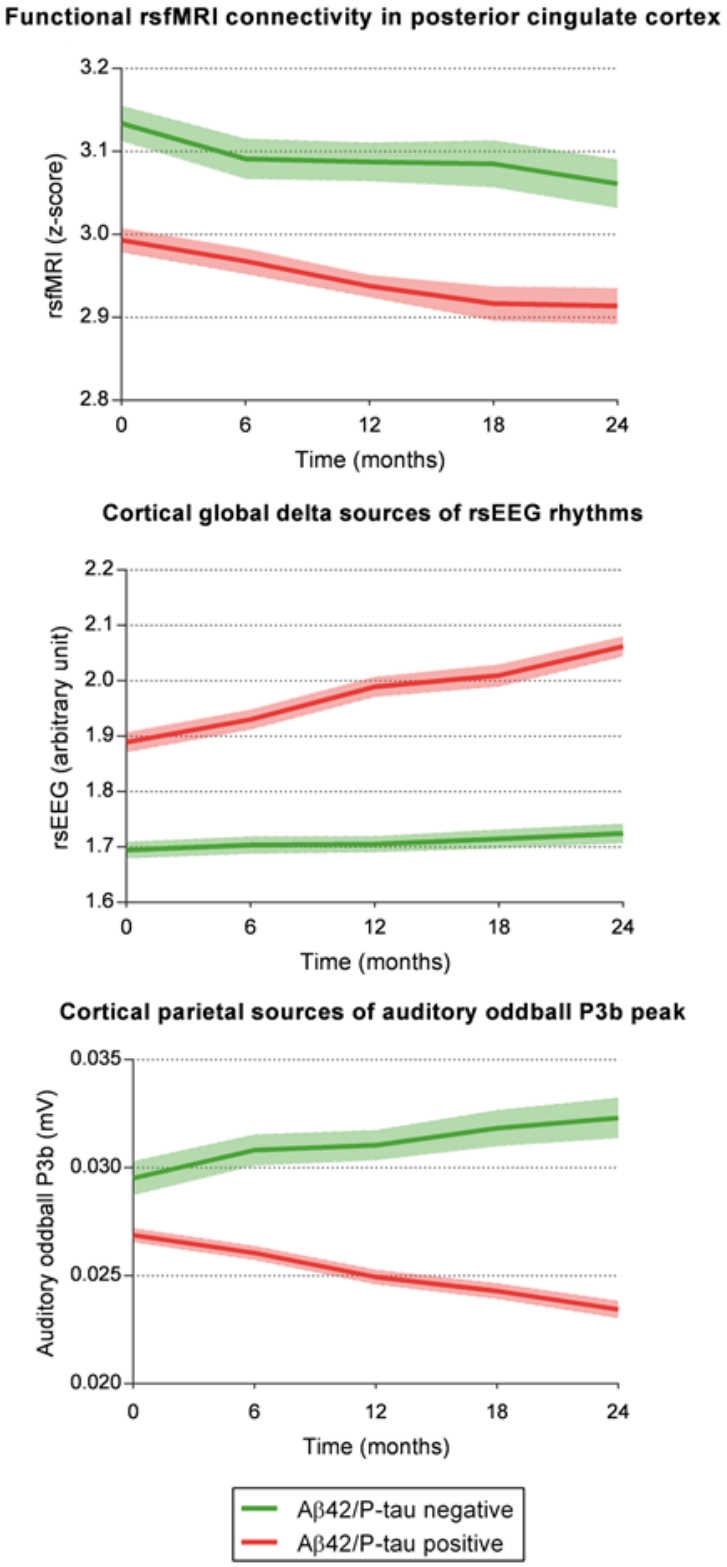
Functional rsfMRI connectivity in posterior cingulate cortex
rsfMRI (z-score)
3.2
3.1
3.0
2.9
2.8
0
6
12
18
24
Time (months)
Cortical global delta sources of rsEEG rhythms
rsEEG (arbitrary unit)
2.2
2.1
2.0
1.9
1.8
1.7
1.6
0
6
12
18
24
Time (months)
Cortical parietal sources of auditory oddball P3b peak
Auditory oddball P3b (mV)
0.035
0.030
0.025
0.020
0
6
12
18
24
Time (months)
Aβ42/P-tau negative
Aβ42/P-tau positive

Figure 2

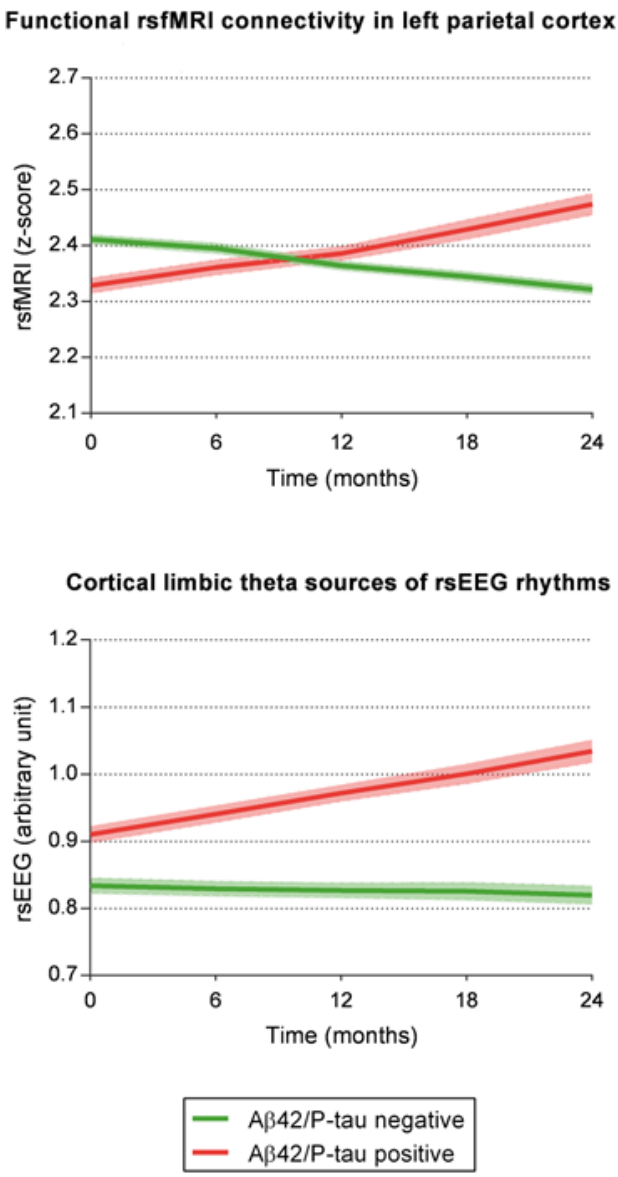
Functional rsfMRI connectivity in left parietal cortex
rsfMRI (z-score)
2.7
2.6
2.5
2.4
2.3
2.2
2.1
0
6
12
18
24
Time (months)
Cortical limbic theta sources of rsEEG rhythms
rsEEG (arbitrary unit)
1.2
1.1
1.0
0.9
0.8
0.7
0
6
12
18
24
Time (months)
Aβ42/P-tau negative
Aβ42/P-tau positive